

Thermodynamics of CeSiO₄: Implications for Actinide Orthosilicates

Andrew C. Strzelecki, Clement Bourgeois, Kyle W. Kriegsman, Paul Estevenon, Nian Wei, Stephanie Szenknect, Adel Mesbah, Di Wu, Rodney C. Ewing, Nicolas Dacheux, and Xiaofeng Guo*

Cite This: *Inorg. Chem.* 2020, 59, 13174–13183

Read Online

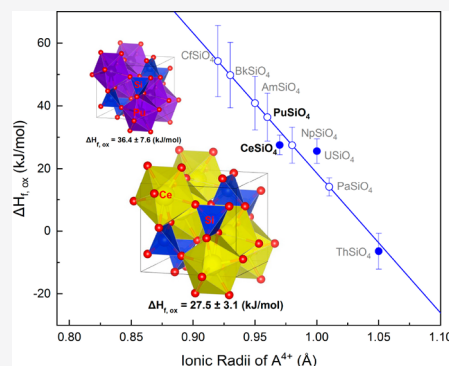
ACCESS |

Metrics & More

Article Recommendations

Supporting Information

ABSTRACT: Zircon (ZrSiO₄, *I*₄₁/*amd*) can accommodate actinides, such as thorium, uranium, and plutonium. The zircon structure has been determined for several of the end-member compositions of other actinides, such as plutonium and neptunium. However, the thermodynamic properties of these actinide zircon structure types are largely unknown due to the difficulties in synthesizing these materials and handling transuranium actinides. Thus, we have completed a thermodynamic study of cerium orthosilicate, stetitite (CeSiO₄), a surrogate of PuSiO₄. For the first time, the standard enthalpy of formation of CeSiO₄ was obtained by high temperature oxide melt solution calorimetry to be -1971.9 ± 3.6 kJ/mol. Stetitite is energetically metastable with respect to CeO₂ and SiO₂ by 27.5 ± 3.1 kJ/mol. The metastability explains the rarity of the natural occurrence of stetitite and the difficulty of its synthesis. Applying the obtained enthalpy of formation of CeSiO₄ from this work, along with those previously reported for USiO₄ and ThSiO₄, we developed an empirical energetic relation for actinide orthosilicates. The predicted enthalpies of formation of AnSiO₄ are then determined with a discussion of future strategies for efficiently immobilizing Pu or minor actinides in the zircon structure.



1. INTRODUCTION

The fate of actinides from spent nuclear fuel discharged from reactors, the actinide-containing waste separated by chemical processing of nuclear fuels, and plutonium from dismantled nuclear weapons has raised several daunting environmental issues.¹ Currently, many countries are investigating solid matrices to immobilize the actinides prior to permanent disposal.² The immobilization step is typically accomplished by either vitrification or cementation, while permanent disposal is completed by either placement in a deep-mined geological repository or a deep bore hole.^{3–5} The main concern with this strategy is the long-term safety associated with a disposal system's integrity on time scales that range from thousands to hundreds of thousands of years.⁶ The structural and chemical stability of ceramics has been ascertained by studies of minerals, such as garnet, pyrochlore, zircon, zirconolite, apatite, and monazite,^{7–15} which are all known to be able to incorporate Th and U over geologic time scales that stretch well beyond 1 million years.¹⁶ Thus, the use of these mineral structure “analogues” as potential ceramic-based waste hosts for the permanent immobilization of actinides and long-lived fission products has been the subject of considerable research over the past several decades.^{17–23}

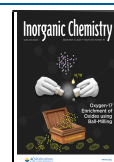
Among the single-phase waste forms, one of the crystalline ceramic candidates for actinide immobilization is zircon (ZrSiO₄, *I*₄₁/*amd*).^{13,14,24} This is a direct result of zircon being an extremely durable mineral with a high loading of actinides and lanthanides.²⁵ The durability of zircon is demonstrated through its high insolubility under a variety of

geochemically relevant conditions^{26–28} (i.e., high-pressure and -temperature environments and highly saline brines), even retaining these properties of insolubility as it undergoes metamictization,^{13,23,25} and a high physical toughness as the mineral grains are shown to endure the abrasive nature of weathering and erosional processes.²⁹

Furthermore, zircon has been reported to readily allow for the substitution of Pu into its structure and has been identified as a key phase for Pu in the “lavas” at the Chernobyl Nuclear Power Plant.^{21,30–33} The synthesis of a pure Pu end-member orthosilicate (PuSiO₄) possessing the zircon structure was reported by Keller in 1963 through hydrothermal synthetic techniques;³⁴ however, questions remain about the overall purity and the extreme difficulty of such a synthesis.³⁵ Also, there could be a miscibility gap within the (Zr,Pu)SiO₄ system, as is evidenced by the substitution of Pu into zircon becoming increasingly more difficult when exceeding 10 wt % Pu.^{15,36,37} This is most likely attributed to the thermodynamically unfavorable formation of PuSiO₄ from its binary oxides, PuO₂ and SiO₂, which also indicates the instability Pu introduces into the zircon structure for the following solid solution reaction: $x\text{Pu}^{4+} + \text{ZrSiO}_4 \rightarrow [\text{Pu}_x\text{Zr}_{(1-x)}\text{SiO}_4] +$

Received: May 20, 2020

Published: September 1, 2020



$x\text{Zr}^{4+}$. This hypothesis is supported by the recent work of Estevenon et al. in 2020, where they found that the hydrothermal conditions under which a pure PuSiO_4 may form are extremely limited, with PuSiO_4 as the minor product and PuO_2 and SiO_2 being the major phases.³⁵ Thus, due to the challenge of obtaining pure PuSiO_4 and the safety precautions in handling of transuranium-bearing orthosilicates, our experiments were conducted using CeSiO_4 . Cerium was selected as the surrogate for Pu, due to the similarity in structure, and the ionic radii of the A-site cations and chemical properties (i.e., multiple valence states).^{38–41} Ce^{4+} in the eight-coordination environment has an ionic radius of 0.97 Å, which is very close to that of eight-coordinated Pu^{4+} (0.96 Å);⁴² therefore, Ce in the solid-state system has been used to simulate Pu. Pure synthetic CeSiO_4 has been successfully prepared by both direct and indirect hydrothermal methods in 2019^{43,44} and has been used for the thermodynamic study in this paper.

We have measured the thermodynamic property of CeSiO_4 for the first time. The significance is 2-fold. First, it has been well accepted that an empirical thermodynamic relation exists within isostructural ceramic materials⁴⁵ such that the enthalpy of formation (ΔH_f) for the ceramic phase can be correlated with the ionic radii of metal cations.⁴⁶ Thus, given the measured ΔH_f of orthosilicates, one may predict the ΔH_f of an unknown phase (i.e., PuSiO_4) through linear extrapolations.⁴⁷ This method enables the evaluation of the impact of Pu and minor actinides on the zircon structure from a thermodynamic perspective. Previously, thermodynamic parameters for coffinite (USiO_4) and thorite (ThSiO_4), compounds that are isostructural to zircon, have been determined experimentally.^{1,8,48} Coffinite was found to be metastable, as evidenced by its positive enthalpy of formation from oxides ($\Delta H_{f,\text{ox}} = 25.6 \pm 3.9$ kJ/mol⁴⁸) measured by Guo et al. using high temperature oxide melt solution calorimetry and the positive Gibbs free energy of formation ($\Delta G_{f,\text{ox}} = 20.6 \pm 5.2$ kJ/mol⁴⁹) determined by Szenknect et al. from solubility studies. The metastability of coffinite directly explains the difficulty associated with its synthesis, such that one cannot simply prepare coffinite by a conventional solid-state reaction.⁵⁰ However, thorite is relatively easier to synthesize by various solid-state and aqueous-chemistry methods,^{51–54} despite the ionic similarity in Th^{4+} (1.05 Å) and U^{4+} (1.00 Å),⁴² and the less difficult synthesis is consistent with its negative value of $\Delta H_{f,\text{ox}}$, -6.4 ± 5.7 kJ/mol.⁸ Additionally, Ferriss et al. in 2010 performed density functional theory (DFT) calculations³⁷ to predict the ΔH_f values of CeSiO_4 , ThSiO_4 , USiO_4 , and PuSiO_4 . The DFT results predict values in good agreement with those of ThSiO_4 ,⁸ USiO_4 ,⁴⁸ and CeSiO_4 from this work.

Second, the natural mineral occurrence of CeSiO_4 , stetindite, was discovered in 2009 in a granitic pegmatite in Norway.⁵⁵ However, there have been no studies of its thermodynamic stability. Thus, the first determination of ΔH_f for CeSiO_4 provides a basis for understanding the geochemical factors leading to the formation of this relatively rare mineral.

2. EXPERIMENTAL METHODS

2.1. Sample Synthesis and Characterization. CeSiO_4 samples were synthesized by the hydrothermal method from a Ce(III)-silicate solid precursor according to the protocol described by Estevenon et al.⁴⁴ A stoichiometric mixture of CeO_2 (Sigma-Aldrich, particle size of <5 μm) and SiO_2 (Sigma-Aldrich, 10–20 nm) was mechanically milled (30 Hz, 1 h) with a Retsch MM 200 vibration mill mixer in a

tungsten carbide milling vessel. This mixture was pelletized by uniaxial pressing under 5 MPa at room temperature and then heated at 1350 °C under a reductive atmosphere ($\text{Ar}/4\% \text{H}_2$) to prepare A- $\text{Ce}_2\text{Si}_2\text{O}_7$ (tetragonal system, space group $P4_1$). Then, 200 mg of A- $\text{Ce}_2\text{Si}_2\text{O}_7$ was placed in contact with 4 mL of a 0.75 M HNO_3 solution (prepared by dilution of ACS grade 70% HNO_3 , Sigma-Aldrich), and the pH of that solution was then adjusted to 7.0 using a freshly prepared NaOH solution (from ACS grade NaOH pellets, Sigma-Aldrich). This mixture was hydrothermally treated for 7 days at 150 °C under an air atmosphere in 23 mL Teflon-lined Parr autoclaves. The final product was separated from the aqueous solution by centrifugation, washed twice with deionized water and once with ethanol, and then dried overnight at 60 °C. The final CeSiO_4 powder sample was then well characterized by complementary characterization techniques. A summary of the techniques and the resulting data are presented in the Supporting Information, with a more detailed description of the characterization being found in the previous work of Estevenon et al.⁴⁴ These techniques included X-ray diffraction (XRD) (Figure S1), Fourier transform infrared spectroscopy (FTIR) (Figure S2), Raman (Figure S3), X-ray absorption near edge structure (XANES) (Figure S4), extended X-ray absorption fine structure (EXAFS) (Figure S5), and scanning electron microscopy (SEM) (Figure S6). The results of all of these techniques allowed us to confirm that the material that was investigated through the calorimetric techniques used and presented in this study was CeSiO_4 from a chemical point of view. The whole Ce was present as a tetravalent oxidation state, and the overall structure belonged to space group $I4_1/amd$.

2.2. Thermogravimetric Analysis Coupled with Differential Scanning Calorimetry (TGA-DSC). The TGA-DSC measurements were performed on a Setaram SetSYS 2400 thermogravimetric differential scanning calorimeter, where CeSiO_4 was heated from 28 to 1200 °C, with a heating rate of 10 °C/min, under a flowing N_2 atmosphere (20 mL/min). The temperature and sensitivity of the instrument were calibrated by heating indium, tin, lead, zinc, and aluminum across their fusion point repeatedly at temperature change rates of 5, 10, 15, and 20 °C/min. The signals of each phase transition were then calibrated against the known heats of fusion for the metals.

2.3. High Temperature Oxide Melt Solution Calorimetry. The enthalpy of the drop solution (ΔH_{ds}) was directly measured by a Setaram AlexSYS-1000 Calvet-type calorimeter. The calibration of the instrument was conducted by performing transpose temperature drops using solid pieces of $\alpha\text{-Al}_2\text{O}_3$ and Pt. Powdered samples were hand pressed into pellets, with masses between 3 and 5 mg, and dropped from room temperature into a molten solvent of sodium molybdate ($\text{Na}_2\text{O}\cdot\text{MoO}_3$) contained in a Pt crucible at 700 °C. The calorimeter chambers were continuously flushed with O_2 gas at a rate of ~ 100 mL/min to facilitate a constant gas environment above the solvent. The $\text{Na}_2\text{O}\cdot\text{MoO}_3$ melt is slightly oxidative^{56,57} and will maintain a redox environment that will keep all of the dissolved Ce in the melt as Ce^{4+} .^{58–60} Flushing of O_2 gas above the solvent also further aids in maintaining an oxidative solvent environment, by oxidizing any low-valence Mo to Mo^{6+} . In addition, the $\text{Na}_2\text{O}\cdot\text{MoO}_3$ solvent dissolves refractory elements, such as Ce, but is relatively chemically inert to silicon (Si).^{48,58,60,61} Therefore, the solvent saturation method⁶² was used to correctly account for the energy associated with all of the Si in the stetindite. This was accomplished by saturating 15 g of $\text{Na}_2\text{O}\cdot\text{MoO}_3$ with 100 mg of silica gel prior to the experiments as the solvent will no longer dissolve any SiO_2 but instead will precipitate out as cristobalite at 700 °C. All of the calibration and methodology employed in this study are further described in more detail in previous reports.^{11,48,58,62–65}

3. RESULTS AND DISCUSSION

3.1. Thermogravimetric Analysis Coupled with Differential Scanning Calorimetry (TGA-DSC). Thermogravimetric analysis (TGA) of CeSiO_4 showed two temperatures of mass loss (Figure 1). The first mass loss of 3.20% occurs from room temperature to 900 °C and is associated with the

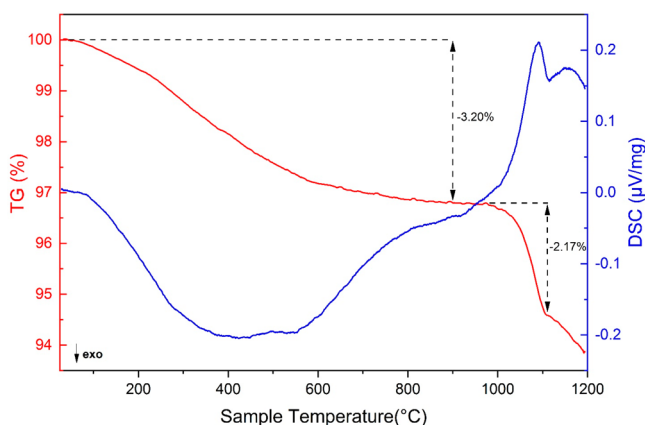


Figure 1. TGA-DSC curve obtained from $\text{CeSiO}_4 \cdot 0.43\text{H}_2\text{O}$ (sample mass of 4.5220 ± 0.0005 mg) upon heating to 1200 °C under a N_2 atmosphere.

removal of surface water and structural water. The water content of the synthetic CeSiO_4 was quantified from the TGA result leading to the chemical formula $\text{CeSiO}_4 \cdot 0.43\text{H}_2\text{O}$, which also resembles the hydrated form of synthetic USiO_4 prepared by hydrothermal methods.⁴⁸ The origins and location of water within zircon structural materials has been vigorously debated in the literature.^{17,52,66–71} The observation of a continual mass until 900 °C shows that a portion of the water associated with CeSiO_4 is energetically strongly associated with the material, with the adsorbed water on the surface leaving the sample below 200 °C. This conclusion of strongly associated water is consistent with the previous observations of excess water associated with both natural and synthetic coffinite samples (USiO_4).^{17,48} However, the origin of such excess water in coffinite is not simple and still subject to debate as both infrared spectroscopic and X-ray diffraction studies have ruled out the water being structural.^{17,52,66–70} One prevailing theory of how water is associated with natural zircons is in the form of OH- and various Zr- or Si-related vacancies.⁷¹ Such hydroxide groups would have been evidenced in the $3000\text{--}3500$ cm^{-1} IR region.⁷² However, they were not detected by FTIR (Figure S2). They would further require a charge substitution of Ce^{4+} to Ce^{3+} ; the latter was not present in the XANES spectra (Figure S4). Lastly, the EXAFS (Figure S5) of the material showed that the coordination environment of the elements was in agreement with that observed in zircon structural material, with no vacancies or OH^- being found to contribute. Such water that was energetically strongly associated, but not structural and not readily visible through FTIR or XRD, could be confined as molecular water inside channels along the $[001]$ direction in the zircon structure.^{17,70,73} This hypothesis offers an explanation for why the water was observed as molecular and not structural.⁶⁹

The second mass loss (2.17%) from 980 to 1110 °C was associated with the release of $1/4$ mol of O_2 in association with the partial reduction of Ce^{4+} to Ce^{3+} , resulting in the cerium(III) disilicate phase, $\text{A-Ce}_2\text{Si}_2\text{O}_7$, under an inert atmosphere. This was further supported by the corresponding endothermic heat flow indicated by DSC. The decomposition temperature was much higher than 700 °C, at which the oxide melt solution calorimetry was conducted. Thus, we conclude that the decomposition had no bearing on the final thermochemical results.

3.2. Enthalpy of Formation of CeSiO_4 . The hydrothermally prepared CeSiO_4 sample used in this study exhibits a hydrated composition similar to that of the analogous synthetic USiO_4 prepared by similar hydrothermal techniques.^{48,74} To ensure the quality of the obtained enthalpy of formation, we followed the previously developed method for hydrated minerals (e.g., coffinite⁴⁸) and performed two sets of high temperature oxide melt solution calorimetry experiments. The first set of these experiments was performed using the sample as is, with a chemical formula of $\text{CeSiO}_4 \cdot 0.43\text{H}_2\text{O}$. Through these experiments, the enthalpy of the drop solution (ΔH_{ds}) of $\text{CeSiO}_4 \cdot 0.43\text{H}_2\text{O}$ was found to be 95.36 ± 3.52 kJ/mol (Table 1). The second set of experiments was performed after the

Table 1. Thermochemical Cycles Used for Calculations of the Enthalpy of Formation from Binary Oxides and the Standard Enthalpy of Formation of Stetindite Based on the Data of Drop Solution Calorimetry in Molten Sodium Molybdate Saturated with Amorphous Silica at 25 °C

reaction	ΔH (kJ/mol)
(1) $\text{CeSiO}_4 \cdot 0.43\text{H}_2\text{O}_{(s, 25\text{ }^\circ\text{C})} \rightarrow \text{CeO}_{2(\text{sln}, 700\text{ }^\circ\text{C})} + \text{SiO}_{2(\text{cristobalite}, 700\text{ }^\circ\text{C})} + 0.43\text{H}_2\text{O}_{(\text{g}, 700\text{ }^\circ\text{C})}$	$\Delta H_1 = 95.36^a \pm 3.52^b$ (3) ^c
(2) $\text{CeSiO}_{4(s, 25\text{ }^\circ\text{C})} \rightarrow \text{CeO}_{2(\text{sln}, 700\text{ }^\circ\text{C})} + \text{SiO}_{2(\text{cristobalite}, 700\text{ }^\circ\text{C})}$	$\Delta H_2 = 92.88 \pm 3.40$ (2)
(3) $\text{CeO}_{2(s, 25\text{ }^\circ\text{C})} \rightarrow \text{CeO}_{2(\text{sln}, 700\text{ }^\circ\text{C})}$	$\Delta H_3 = 74.37 \pm 0.75^{58}$ (66)
(4) $\text{SiO}_{2(\text{quartz}, 25\text{ }^\circ\text{C})} \rightarrow \text{SiO}_{2(\text{cristobalite}, 700\text{ }^\circ\text{C})}$	$\Delta H_4 = 43.54 \pm 0.60^{58}$ (3)
(5) $\text{Ce}_{(s, 25\text{ }^\circ\text{C})} + \text{O}_{2(\text{g}, 25\text{ }^\circ\text{C})} \rightarrow \text{CeO}_{2(s, 25\text{ }^\circ\text{C})}$	$\Delta H_5 = -1088.7 \pm 1.5^{119}$
(6) $\text{Si}_{(s, 25\text{ }^\circ\text{C})} + \text{O}_{2(\text{g}, 25\text{ }^\circ\text{C})} \rightarrow \text{SiO}_{2(\text{quartz}, 25\text{ }^\circ\text{C})}$	$\Delta H_6 = -910.7 \pm 1.0^{119}$
(7) $\text{H}_2\text{O}_{(l, 25\text{ }^\circ\text{C})} \rightarrow \text{H}_2\text{O}_{(\text{g}, 700\text{ }^\circ\text{C})}$	$\Delta H_7 = 69.0^{119}$
(8) $\text{H}_2\text{O}_{(l, 25\text{ }^\circ\text{C})} \rightarrow \text{H}_2\text{O}_{(\text{cr}, 25\text{ }^\circ\text{C})}$	$\Delta H_8 = -80.0^{48}$
Enthalpy of the Drop Solution Corrected for the Proper Molar Mass of the Partially Hydrated Sample	
(9) $\text{CeSiO}_4 \cdot 0.025\text{H}_2\text{O}_{(s, 25\text{ }^\circ\text{C})} \rightarrow \text{CeO}_{2(\text{sln}, 700\text{ }^\circ\text{C})} + \text{SiO}_{2(\text{cristobalite}, 700\text{ }^\circ\text{C})} + 0.025\text{H}_2\text{O}_{(\text{g}, 700\text{ }^\circ\text{C})}$	$\Delta H_9 = -92.48 \pm 3.42$
Corrected Enthalpy of the Drop Solution Value Assuming Water Is Strongly Bonded	
(10) $\Delta H_{\text{ds}}(\text{CeSiO}_4) = \Delta H_{10} = \Delta H_9 - 0.025(\Delta H_6 + \Delta H_{\text{ds}}) = 88.7 \pm 3.4$	ΔH_7
Enthalpy of Formation of Stetindite from CeO_2 and SiO_2 (quartz) Assuming Water Is Strongly Bonded	
(11) $\Delta H_{\text{f,ox}}(\text{CeSiO}_4) = \Delta H_{11} = -\Delta H_{10} + \Delta H_3 + \Delta H_{\text{f,ox}} = 29.2 \pm 3.5$	ΔH_4
Standard Enthalpy of Formation of Stetindite Assuming Water Is Strongly Bonded	
(12) $\Delta H_{\text{f}}^\circ(\text{CeSiO}_4) = \Delta H_{11} + \Delta H_4 + \Delta H_5$	$\Delta H_{\text{f}}^\circ = -1970.2 \pm 4.0$
Enthalpy of Formation of Dehydrated Stetindite from CeO_2 and SiO_2 (quartz)	
(13) $\Delta H_{\text{f,ox}}(\text{CeSiO}_4) = \Delta H_{13} = -\Delta H_2 + \Delta H_3 + \Delta H_{\text{f,ox}} = 25.0 \pm 3.5$	ΔH_4
Standard Enthalpy of Formation of Stetindite	
(14) $\Delta H_{\text{f}}^\circ(\text{CeSiO}_4) = \Delta H_{13} + \Delta H_4 + \Delta H_5$	$\Delta H_{\text{f}}^\circ = -1974.2 \pm 4.0$

^aAverage. ^bTwo standard deviations of the average value. ^cNumber of measurements.

sample was fully dehydrated. The dehydration of the sample was accomplished by heating pelletized samples (3–5 mg) for 2 h under an inert atmosphere of N_2 to 800 °C. Samples were then stored at room temperature under a N_2 atmosphere prior to being dropped to avoid any potential water readsorption. All of the experimental parameters and materials exactly mirrored those utilized for the hydrated sample outlined above in Experimental Methods. The resulting enthalpy of drop

solutions (ΔH_{ds}) determined by these experiments was 92.88 ± 3.40 kJ/mol (Table 1), slightly less endothermic than that from the first experiment. This is reasonable because the thermal dehydration leads to the positive contribution to the ΔH_{ds} value. However, the difference, 2.48 kJ/mol, is unexpectedly small. The small hydration enthalpic value could be due to the partial dehydration of $\text{CeSiO}_4 \cdot 0.43\text{H}_2\text{O}$ during dropping before it reached the reaction chamber where the measurements were taken. AlexSYS-1000 has an inhomogeneous temperature profile, with >60 cm above the reaction chamber being maintained at around 650 °C. Rapid dehydration could occur,^{75,76} and the composition of the resulting sample detected by the thermophiles was estimated from the TGA result to be $\text{CeSiO}_4 \cdot 0.025\text{H}_2\text{O}$.

The ΔH_{ds} for such partially hydrated sample must be then corrected to account for the additional energetics related with the associated water. As stated above, a portion of the water is strongly bonded to CeSiO_4 as the TGA data showed an extended mass loss until 900 °C. Using an integral adsorption enthalpy of -80 kJ/mol per mole of H_2O (-44 kJ/mol for “free water”) for the adsorbed water, which was observed in the alumina and titania^{77–79} and used to estimate the hydration energy of coffinite,⁴⁸ one may derive the corrected ΔH_{ds} for anhydrous CeSiO_4 to be 88.7 ± 3.4 kJ/mol and $\Delta H_{\text{f,ox}}$ to be 29.2 ± 3.5 kJ/mol (Table 1). While the direct measurement of anhydrous CeSiO_4 yields a $\Delta H_{\text{f,ox}}$ of 25.0 ± 3.5 kJ/mol (Table 1), averaging the results of the two experiments yields a $\Delta H_{\text{f,ox}}$ of CeSiO_4 of 27.5 ± 3.1 kJ/mol (Table S1), which is in excellent agreement with the DFT-predicted value, 23.8 kJ/mol.^{37,63} With all of the evidence supporting the idea that water is energetically strongly associated with stettindite, we report that $\Delta H_{\text{f}}^\circ = -1971.9 \pm 3.6$ kJ/mol, which is the first reported standard enthalpy of formation data of stettindite (Table S1).

3.3. Energetic Landscape of End-Member Actinide Orthosilicates. Several empirical methodologies were developed for the prediction of thermodynamic parameters of ceramic compounds. For instance, Chen et al. discovered that both the Gibbs free energies (ΔG_{f}) and enthalpies of formation (ΔH_{f}) of hexavalent uranium minerals could be predicted through the structural-summation technique.⁸⁰ On the contrary, Sverjensky and Molling⁴⁵ established an empirical linear relationship between the free energy of isostructural inorganic solids and the ionic radii of aqueous metal cations. While this model was originally developed for divalent cations, the model has been expanded to include tetravalent cations and its application allowed for the free energies of crystalline solids to be estimated by only having experimental data on a few samples.^{81,82} A very similar empirical linear relationship has been recognized for isostructural inorganic compounds that links the enthalpies of formation with the ionic radii of metal cations.⁴⁶ Many lanthanide- and actinide-bearing isostructural ceramic materials follow this empirical trend, and it has been applied numerous times.^{47,64,83–85}

By using the experimentally determined $\Delta H_{\text{f,ox}}$ of CeSiO_4 (27.5 ± 3.1 kJ/mol), USiO_4 (25.6 ± 3.9 kJ/mol⁴⁸), and ThSiO_4 (-6.4 ± 5.7 kJ/mol⁸) and the ionic radii (angstroms) of metal cations in an 8-fold coordination environment,⁴² a nearly linear trend is found between $\Delta H_{\text{f,ox}}$ and ionic radius r (angstroms), $\Delta H_{\text{f,ox}} = (-446.3 \pm 152.5)r - (464.9 \pm 153.6)$, with an adjusted R^2 of 0.79096. From the obtained linear regression, we obtained the $\Delta H_{\text{f,ox}}$ for the other actinide (Pa, Np, Pu, Am, Bk, and Cf) orthosilicates (Figure 2). The heavier

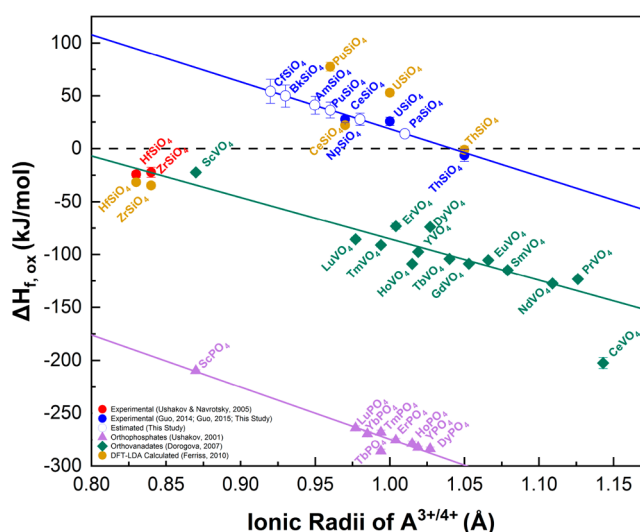


Figure 2. Enthalpy of formation from binary oxides obtained for orthosilicates (ASiO_4), orthovanadates (AVO_4), and orthophosphates (APO_4) that crystallize with the zircon structure ($I4_1/amd$) as a function of the ionic radius of a metal cation (A^{4+} or A^{3+}) in the 8-fold coordination. Data shown as filled blue circles were used to estimate the values for the empty blue circles by means of linear regression. The equation that describes the blue line is $\Delta H_{\text{f,ox}} = (-446.3 \pm 152.5)r - (464.9 \pm 153.6)$, with an adjusted R^2 of 0.79096. Data denoted with orange circles were derived by utilizing the DFT-LDA results for the enthalpy of formation of orthosilicate materials at -273 °C reported by Ferriss et al.,³⁷ in conjunction with the standard enthalpy of formation of quartz¹¹⁹ and AO_2 ¹⁰⁷ ($\text{A} = \text{Ce}, \text{U}, \text{Th}, \text{or Pu}$). This assumes that the energetic contributions from the respective heat capacities are negligible to the overall calculation, so the enthalpy of formation data reported by Ferriss et al. can be treated as approximately equal to standard-state conditions. Data points as purple triangles and green diamonds are for orthophosphates⁵⁹ and orthovanadates,¹⁰⁸ respectively.

transuranic elements (Am, Bk, and Cf) show more lanthanide-like characteristics and, thus, prefer having a trivalent oxidation state.^{86–88} The trivalent oxidation would result in different ionic radii and preferred coordination chemistry.^{89,90} For such trivalent cations to be introduced into the zircon structure, a charge-coupled substitution would be required. Nonetheless, the tetravalent states of the majority of the aforementioned elements are possible through either a transient state as a result of radiation-induced radiolysis^{91–94} or a steady state being stabilized by either ligands or electrochemical methods.^{88,95–97} Both, transient-state and steady-state conditions can be achieved in the unlikely event of a failure of the geological repository and breach in radiological waste canister. Each of these states could be observed under such a hypothetical scenario, if said geological repository is located in a geologic setting where the host lithology is also rich with mineral halides (i.e., halite), such as what is observed at the Waste Isolation Pilot Plant (WIPP) located in New Mexico,^{98,99} and then there would be a supply of radiation, heat, high-ionic strength aqueous solutions,¹⁰⁰ and the silica source from the natural barriers.¹⁰¹ This could cause the dissolution of another ceramic waste form and allow for the formation of an actinide orthosilicate, with such hypothetical conditions being similar to those used in synthesizing PuSiO_4 .³⁵ These actinide orthosilicate could be formed first as colloids, which could impact the actinide mobility and allow their transport over important distances.^{102–105} Thus, here we consider the

Table 2. Enthalpies of Formation from Oxides for Orthosilicate End Members, from Experiments and Calculations at 25 °C

	VIII A ⁴⁺ ionic radii ⁴² (Å)	ΔH_f° for AO ₂ (kJ/mol)	ΔH_f° for ASiO ₄ (kJ/mol)	$\Delta H_{f,ox,25\text{ }^\circ\text{C}}$ for ASiO ₄ (kJ/mol)
zircon	0.84	-1100.6 ± 1.7^a	-2035.5 ± 3.4^a	-24.2 ± 2.8^a
hafnon	0.83	-1117.6 ± 1.6^a	-2050.3 ± 5.1^a	-22.3 ± 4.7^a
stetindite	0.97	-1090.4 ± 1.0^b	-1971.9 ± 3.6^e	27.5 ± 3.1^e
thorite	1.05	-1226.4 ± 3.5^b	-2143.5 ± 6.8^e	-6.4 ± 5.7^e
PaSiO ₄	1.01	-1107.0 ± 15.0^b	-2003.6 ± 15.1^f	14.1 ± 2.9^f
coffinite	1.00	-1085.0 ± 1.0^b	-1970.0 ± 4.2^d	25.6 ± 3.9^d
NpSiO ₄	0.98	-1078.5 ± 2.7^b	-1961.7 ± 4.1^f	27.5 ± 5.7^f
PuSiO ₄	0.96	-1055.8 ± 1.0^b	-1930.1 ± 4.1^f	36.4 ± 7.6^f
AmSiO ₄	0.95	-932.2 ± 3.0^b	-1802.0 ± 5.3^f	40.9 ± 8.5^f
BkSiO ₄	0.93	not available	not available	49.8 ± 10.4^f
CfSiO ₄	0.92	not available	not available	54.3 ± 11.3^f

^aFrom ref 120. ^bFrom ref 107. ^cFrom ref 8. ^dFrom ref 48. ^eExperimentally derived in this study. ^fCalculated in this study.

possible tetravalent states of these heavy transuranic elements and their potential impact on the structural stability.

As the thermodynamic stability of any given material is dictated by ΔG_f , one needs $\Delta G_f = \Delta H_f - T\Delta S_f$ with knowing the appropriate entropy (ΔS_f) value besides ΔH_f to evaluate the overall stability. However, under the standard condition and room temperature, the entropic term is small. This is evidenced by taking coffinite as an example. The ΔG_f of coffinite was determined through solubility studies to be -1867.6 ± 3.2 kJ/mol,⁴⁹ and its ΔH_f was determined by high temperature drop oxide melt calorimetry to be -1970.0 ± 4.2 kJ/mol.⁴⁸ At 25 °C, $T\Delta S_f = -0.344$ kJ mol⁻¹ K⁻¹ \times 298.15 K = 102.6 kJ/mol. Hence, under the standard condition, enthalpy alone can be used to approximately discuss the stability of actinide orthosilicates and represent the energetic landscape (Figure 2). The regression of measured $\Delta H_{f,ox}$ leads to an almost linear trend. The extrapolated results based on such linear trend are in good agreement with those reported in a previous computational study.³⁷ The result of the linear regression is summarized in Table 2 and plotted in Figure 2. Only ThSiO₄ has a negative formation enthalpy (-6.4 ± 5.7 kJ/mol),⁸ while all others are expected to be thermodynamically metastable with respect to their binary oxides (AnO₂ and SiO₂). The favorable formation of ThSiO₄ could be a result of it having the lowest ionic potential (Z/r) of 3.81 that allows Th⁴⁺ to be stabilized in the zircon structure, whereas USiO₄, CeSiO₄, and PuSiO₄ having larger ionic potentials of 4.00, 4.12, and 4.17, respectively, are more difficult to stabilize in the zircon structure. That said, the $\Delta H_{f,ox}$ of ThSiO₄ follows the linear trend established in this work and does not appear as an exception to the general rule.

The predictions in Figure 2 are consistent with the reported difficulty in synthesizing pure PuSiO₄,³⁵ which has a predicted $\Delta H_{f,ox}$ value of 36.4 ± 7.6 kJ/mol. These results indicate the use of the zircon structure to perform the specific immobilization of Pu or other minor actinides require target synthesis strategies that should disfavor the formation of associated oxides. As both coffinite and stetindite are found to have positive $\Delta H_{f,ox}$ values, the synthetic conditions of their formation could be highly informative for such strategies. Both of them have been discovered in nature under hydrothermal conditions, and their synthetic analogues have been prepared by tailoring synthetic routes to avoid the formation of thermodynamically more favorable mixture of oxides.^{43,44,50,53,106} In particular, the kinetics needed to oxidize the Ce³⁺ intermediate complex⁴³ or a Ce³⁺-bearing solid⁴⁴ to Ce⁴⁺ was reached only under hydrothermal conditions, leading

to the formation synthetic stetindite.^{43,44} In addition, taking the $\Delta H_{f,ox}$ calculated through the linear regression, we also report the predicted ΔH_f° values for PaSiO₄, NpSiO₄, PuSiO₄, AmSiO₄, etc. (Table 2), by using the ΔH_f° of the respected AnO₂¹⁰⁷ as the auxiliary data. The overall $\Delta H_{f,ox}$ is shown to be thermodynamically unfavorable for the major transuranic elements. Historically, only Am-orthosilicate has been successfully synthesized and reported by Keller in 1963, with only perspective synthetic routes proposed for CmSiO₄ and BkSiO₄.³⁴

The zircon structure type includes other crystalline ceramics. The lanthanide orthovanadate (LnVO₄) minerals wakefieldite and dreyerite, the heavy rare earth orthophosphate (HREE-PO₄) mineral xenotime, and the lanthanide orthoarsenate (LnAsO₄) mineral chernovite all share the zircon structure.¹⁷ As the enthalpies of formation of the orthophosphate and orthovanadate materials have been reported in the literature,^{59,108} they are also included in Figure 2 to detect any other trends across the isostructural family. This led to another important observation of the energetic landscape of orthosilicates in that both zircon and hafnon (HfSiO₄) are “outliers” of the predicted trend. We hypothesize that there could be a separate trend for transitional metal orthosilicates due to the structural difference in that both Zr⁴⁺ and Hf⁴⁺ are smaller cations (0.84 and 0.83 Å, respectively). This is further supported by the observation that both of these materials follow the orthovanadate trend line, which are comparable in both energetics and unit cell volume to ScVO₄. This observation, however, does not exclude the possibility of zircon and hafnon being outliers as a result of the fundamental bonding difference in d orbitals versus f orbitals.¹⁰⁹ Lastly, these two trends for transition metal and lanthanide/actinide orthosilicates disagree with the previously reported actinide orthosilicate energetic landscape.¹¹⁰ The discrepancy is attributed to the inaccuracy of the ΔH_{ds} for thorite as a result of incomplete dissolution of the single-crystal sample and the inconclusive ΔH_{ds} for coffinite in the early experiments, which we have discussed in a previous work.⁴⁸ The experimentally derived energetic trend fully agrees with the calculated values reported by the DFT-LDA study³⁷ (Figure 2), which likewise shows that both zircon and hafnon deviate from the linear trend.

3.4. Strategic Analysis of Immobilizing Pu or Other Actinides in the Zircon Structure. Although the pure actinide orthosilicate end members were calculated to have a positive $\Delta H_{f,ox}$, the question of whether any intermediate compositions from MSiO₄ (M = Zr or Hf) and AnSiO₄ (An =

Th, U, Np, Pu, etc.) end members can lead to thermodynamically favorable solid solutions for waste form applications should be investigated. Using MSiO_4 -based solid solutions to strategically accommodate actinides has two different types of advantages. First, it may allow for easier synthesis of actinide-containing orthosilicates, as there could be a potential for cation ordering or polyhedral distortion that could significantly lower the enthalpic penalty for introducing An^{4+} into ZrSiO_4 . Such a phenomenon has already been demonstrated in an uranothorite solid solution ($\text{Th}_{1-x}\text{U}_x\text{SiO}_4$), where the intermediate compositions are stabilized by a negative heat effect of -118.7 kJ/mol.⁸ Second, the application of HfSiO_4 as the end member, instead of ZrSiO_4 , can offer an additional benefit to the waste form as hafnium is a neutron absorber.^{14,19} The soft hydrothermal synthesis of hafnion could be easily modified to incorporate tetravalent actinides.¹¹¹ This soft hydrothermal synthetic technique could also be scalable for industrial application.¹¹² Unfortunately, the introduction of hafnium as a neutron absorber does not imply a reduction in the susceptibility to radiation damage,²¹ a topic that has been extensively studied in the past^{31,113–118} and is still one of the greatest challenges to the utilization of a zircon-based ceramic as a nuclear waste host. However, the introduction of hafnium could allow the incorporation of higher loadings of radionuclides with high specific activity (e.g., plutonium and americium isotopes) in the waste form without any worry of possible criticality.¹⁵

4. CONCLUSIONS

Through thermogravimetric analysis, differential scanning calorimetry, and high temperature oxide melt solution calorimetry, the thermodynamic parameters of stetindite (CeSiO_4) were determined. The results of TGA-DSC showed that CeSiO_4 was hydrated, like USiO_4 .⁴⁸ By performing high temperature oxide melt solution calorimetry on CeSiO_4 , we found the enthalpy of formation ($\Delta H_{f,\text{ox}}$) to be 27.5 ± 3.1 kJ/mol, confirming its metastability with respect to its binary oxides. The strong endothermic heat of formation accounts for the difficulty in synthesizing this phase in addition to the overall rarity of stetindite in nature. The overall enthalpy of formation was found to be thermodynamically favorable: $\Delta H_f^\circ = -1971.9 \pm 3.6$ kJ/mol. Exploiting the empirically derived linear trend between the enthalpy of formation and the ionic cation radius enabled the prediction of the ΔH_f° values of some unknown actinide silicates AnSiO_4 ($\text{An} = \text{Np}, \text{Pu}, \text{Am}, \text{Bk}, \text{or Cf}$). These high endothermic formation enthalpies provide an explanation for the difficulties in their synthesis, particularly the attempts to obtain pure PuSiO_4 , which was performed by Estevenon et al.³⁵ using hydrothermal methods. Indeed, it appears to be difficult according to a predicted $\Delta H_{f,\text{ox}}$ value of 36.4 ± 7.6 kJ/mol. Furthermore, the synthesis of minor actinides possessing the zircon structure, such as AmSiO_4 , should be even more difficult to synthesize as they are all found to be more energetically uphill than PuSiO_4 , with all being estimated to have $\Delta H_{f,\text{ox}}$ values of >40 kJ/mol. Lastly, we propose that some Zr-An or Hf-An orthosilicate systems may be thermodynamically favored by possible negative mixing enthalpies due to the short-range ordering of the two metal cations that can be engineered to increase the loadings of actinides in the zircon or hafnion structure type, which have a relatively large stability field.

■ ASSOCIATED CONTENT

Supporting Information

The Supporting Information is available free of charge at <https://pubs.acs.org/doi/10.1021/acs.inorgchem.0c01476>.

PXRD, FTIR, Raman, XANES, EXAFS, SEM, and thermochemical tables (PDF)

■ AUTHOR INFORMATION

Corresponding Author

Xiaofeng Guo – Department of Chemistry, Alexandra Navrotsky Institute for Experimental Thermodynamics, and Materials Science and Engineering, Washington State University, Pullman, Washington 99164, United States; orcid.org/0000-0003-3129-493X; Email: x.guo@wsu.edu

Authors

Andrew C. Strzelecki – Department of Chemistry, Alexandra Navrotsky Institute for Experimental Thermodynamics, and Materials Science and Engineering, Washington State University, Pullman, Washington 99164, United States

Clement Bourgeois – Department of Chemistry and Alexandra Navrotsky Institute for Experimental Thermodynamics, Washington State University, Pullman, Washington 99164, United States

Kyle W. Kriegsman – Department of Chemistry and Alexandra Navrotsky Institute for Experimental Thermodynamics, Washington State University, Pullman, Washington 99164, United States

Paul Estevenon – ICSM, Univ Montpellier, CNRS, CEA, ENSCM, Bagnols sur Ceze 30207, France; CEA, DES, ISEC, DMRC, Univ Montpellier, Site de Marcoule 30207, France

Nian Wei – Department of Chemistry, Washington State University, Pullman, Washington 99164, United States; College of Physical Science and Technology, Sichuan University, Chengdu 610065, People's Republic of China

Stephanie Szenknect – ICSM, Univ Montpellier, CNRS, CEA, ENSCM, Bagnols sur Ceze 30207, France; orcid.org/0000-0003-3691-3621

Adel Mesbah – ICSM, Univ Montpellier, CNRS, CEA, ENSCM, Bagnols sur Ceze 30207, France; orcid.org/0000-0002-6905-2402

Di Wu – Department of Chemistry, Alexandra Navrotsky Institute for Experimental Thermodynamics, Materials Science and Engineering, and The Gene and Linda Voiland School of Chemical Engineering and Bioengineering, Washington State University, Pullman, Washington 99164, United States; orcid.org/0000-0001-6879-321X

Rodney C. Ewing – Department of Geological Sciences, Stanford University, Stanford, California 94305, United States

Nicolas Dacheux – ICSM, Univ Montpellier, CNRS, CEA, ENSCM, Bagnols sur Ceze 30207, France; orcid.org/0000-0003-1636-1313

Complete contact information is available at:

<https://pubs.acs.org/doi/10.1021/acs.inorgchem.0c01476>

Notes

The authors declare no competing financial interest.

■ ACKNOWLEDGMENTS

This work was supported by the institutional funds from the Department of Chemistry at Washington State University (WSU). A.C.S., K.W.K., and X.G. acknowledge the support by

U.S. Department of Energy, Office of Nuclear Energy, Grant DE-NE0008582. C.B. acknowledges the fellowship provided by Setaram, Inc., for conducting the calorimetric research at WSU. Portions of this research were also supported by collaboration, services, and infrastructure through the Nuclear Science Center User Facility at WSU. The authors also acknowledge the funding support from the Alexandra Navrotsky Institute for Experimental Thermodynamics and the WSU-PNNL Nuclear Science and Technology Institute.

REFERENCES

- (1) Burns, P. C.; Ewing, R. C.; Navrotsky, A. Nuclear Fuel in a Reactor Accident. *Science (Washington, DC, U. S.)* **2012**, *335* (6073), 1184–1188.
- (2) Orlova, A. I.; Ojovan, M. I. Ceramic Mineral Waste-Forms for Nuclear Waste Immobilization. *Materials* **2019**, *12* (16), 2638.
- (3) Goel, A.; McCloy, J. S.; Pokorny, R.; Kruger, A. A. Challenges with Vitrification of Hanford High-Level Waste (HLW) to Borosilicate Glass – An Overview. *J. Non-Cryst. Solids* **2019**, *4*, 100033.
- (4) Wegel, S.; Czempinski, V.; Oei, P.-Y.; Wealer, B. Transporting and Storing High-Level Nuclear Waste in the U.S.-Insights from a Mathematical Model. *Appl. Sci.* **2019**, *9* (12), 2437.
- (5) Weber, W. J.; Navrotsky, A.; Stefanovsky, S.; Vance, E. R.; Vernaz, E. Materials Science of High-Level Immobilization. *MRS Bull.* **2009**, *34* (1), 46.
- (6) Ewing, R. C. Long-Term Storage of Spent Nuclear Fuel. *Nat. Mater.* **2015**, *14* (3), 252–257.
- (7) Guo, X.; Navrotsky, A.; Kukkadapu, R. K.; Engelhard, M. H.; Lanzirrotti, A.; Newville, M.; Ilton, E. S.; Sutton, S. R.; Xu, H. Structure and Thermodynamics of Uranium-Containing Iron Garnets. *Geochim. Cosmochim. Acta* **2016**, *189*, 269–281.
- (8) Guo, X.; Szenknect, S.; Mesbah, A.; Clavier, N.; Poinssot, C.; Wu, D.; Xu, H.; Dacheux, N.; Ewing, R. C.; Navrotsky, A. Energetics of a Uranothorite ($\text{Th}_{1-x}\text{U}_x\text{SiO}_4$) Solid Solution. *Chem. Mater.* **2016**, *28* (19), 7117–7124.
- (9) Guo, X.; Tavakoli, A. H.; Sutton, S.; Kukkadapu, R. K.; Qi, L.; Lanzirrotti, A.; Newville, M.; Asta, M.; Navrotsky, A. Cerium Substitution in Yttrium Iron Garnet: Valence State, Structure, and Energetics. *Chem. Mater.* **2014**, *26* (2), 1133–1143.
- (10) Chung, C. K.; O’Quinn, E. C.; Neufeind, J. C.; Fuentes, A. F.; Xu, H.; Lang, M.; Navrotsky, A. Thermodynamic and Structural Evolution of Mechanically Milled and Swift Heavy Ion Irradiated $\text{Er}_2\text{Ti}_2\text{O}_7$ Pyrochlore. *Acta Mater.* **2019**, *181*, 309–317.
- (11) Helean, K. B.; Navrotsky, A.; Vance, E. R.; Carter, M. L.; Ebbinghaus, B.; Krikorian, O.; Lian, J.; Wang, L. M.; Catalano, J. G. Enthalpies of Formation of Ce-Pyrochlore, $\text{Ca}_{0.93}\text{Ce}_{1.00}\text{Ti}_{2.035}\text{O}_{7.00}$ U-Pyrochlore, $\text{Ca}_{1.46}\text{U}^{4+}_{0.23}\text{U}^{6+}_{0.46}\text{Ti}_{1.85}\text{O}_{7.00}$ and Gd-Pyrochlore, $\text{Gd}_2\text{Ti}_2\text{O}_7$: Three Materials Relevant to the Proposed Waste Form for Excess Weapons Plutonium. *J. Nucl. Mater.* **2002**, *303* (2–3), 226–239.
- (12) Neumeier, S.; Kegler, P.; Arinicheva, Y.; Shelyug, A.; Kowalski, P. M.; Schreinemachers, C.; Navrotsky, A.; Bosbach, D. Thermochemistry of $\text{La}_{1-x}\text{Ln}_x\text{PO}_4$ -Monazites (Ln = Gd, Eu). *J. Chem. Thermodyn.* **2017**, *105*, 396–403.
- (13) Ewing, R. C.; Lutze, W.; Weber, W. J. Zircon: A Host-Phase for the Disposal of Weapons Plutonium. *J. Mater. Res.* **1995**, *10* (2), 243–246.
- (14) Ewing, R. C. Nuclear Waste Forms for Actinides. *Proc. Natl. Acad. Sci. U. S. A.* **1999**, *96* (7), 3432–3439.
- (15) Ushakov, S. V.; Gong, W.; Yagokina, M. M.; Helean, K. B.; Lutze, W.; Ewing, R. C. Solid Solutions of Ce, U, and Th in Zircon. *Ceram. Trans.* **1999**, *93*, 357–363.
- (16) White, W. M. *Isotope Geochemistry*, 1st ed.; John Wiley & Sons, 2015.
- (17) Finch, R. J.; Hanchar, J. M. Structure and Chemistry of Zircon and Zircon-Group Minerals. *Rev. Mineral. Geochem.* **2003**, *53* (1), 1–26.
- (18) McCarthy, G. J.; White, W. B.; Pfoertsch, D. E. Synthesis of Nuclear Waste Monazites, Ideal Actinide Hosts for Geologic Disposal. *Mater. Res. Bull.* **1978**, *13* (11), 1239–1245.
- (19) Ewing, R. C. The Design and Evaluation of Nuclear-Waste Forms: Clues from Mineralogy. *Can. Mineral.* **2001**, *39* (3), 697–715.
- (20) Lutze, W.; Ewing, R. C. *Radioactive Waste Forms for the Future*; North-Holland Physics Publishing: Amsterdam, 1988.
- (21) Ewing, R. C.; Weber, W. J. Actinide Waste Forms and Radiation Effects. In *The Chemistry of the Actinide and Transactinide Elements*; Morss, L. R., Edelstein, N. M., Fuger, J., Eds.; Springer: Dordrecht, The Netherlands, 2010; pp 3813–3887.
- (22) Weber, W. J.; Ewing, R. C. Chapter 10: Ceramic Waste Forms for Uranium and Transuranium Elements. In *Uranium: Cradle to Grave*; Burns, P. C., Sigmon, G. E., Eds.; Mineralogical Association of Canada, 2013; pp 317–336.
- (23) Weber, W. J.; Ewing, R. C.; Vance, E. R.; Gregg, D.; Peugot, S.; Wiss, T. Plutonium in Waste Forms. In *Plutonium Handbook*; Clark, D. L., Geeson, D. A., Hanrahan, R. J., Jr., Eds.; American Nuclear Society, 2019; pp 2349–2422.
- (24) Ewing, R. C.; Weber, W. J.; Clinard, F. W. Radiation Effects in Nuclear Waste Forms for High-Level Radioactive Waste. *Prog. Nucl. Energy* **1995**, *29* (2), 63–127.
- (25) Weber, W. J.; Ewing, R. C.; Lutze, W. Performance Assessment of Zircon as a Waste Form for Excess Weapons Plutonium Under Deep Borehole Burial Conditions. *Mater. Res. Soc. Symp. - Proc.* **1995**, *412*, 25–32.
- (26) McMurdie, H. F.; Hall, F. P. Phase Diagrams for Ceramists: Supplement No. 1. *J. Am. Ceram. Soc.* **1949**, *32*, 154–164.
- (27) Grover, V.; Tyagi, A. K. Preparation and Bulk Thermal Expansion Studies in $\text{M}_{1-x}\text{Ce}_x\text{SiO}_4$ (M = Th, Zr) System, and Stabilization of Tetragonal ThSiO_4 . *J. Alloys Compd.* **2005**, *390* (1–2), 112–114.
- (28) Subbarao, E. C.; Agrawal, D. K.; McKinsty, H. A.; Sallase, C. W.; Roy, R. Thermal Expansion of Compounds of Zircon Structure. *J. Am. Ceram. Soc.* **1990**, *73* (5), 1246–1252.
- (29) Nesse, W. D. *Introduction to Mineralogy*, 2nd ed.; Oxford University Press, 2000.
- (30) Poirot, I. S.; Kot, W. K.; Edelstein, N. M.; Abraham, M. M.; Finch, C. B.; Boatner, L. A. Optical Study and Analysis of Pu^{4+} in Single Crystals of ZrSiO_4 . *Phys. Rev. B: Condens. Matter Mater. Phys.* **1989**, *39* (10), 6388–6394.
- (31) Weber, W. J. Radiation-Induced Defects and Amorphization in Zircon. *J. Mater. Res.* **1990**, *5* (11), 2687–2697.
- (32) Weber, W. J. Alpha-Decay-Induced Amorphization in Complex Silicate Structures. *J. Am. Ceram. Soc.* **1993**, *76* (7), 1729–1738.
- (33) Anderson, E. B.; Burakov, B. E.; Pazukhin, E. M. High-Uranium Zircon from “Chernobyl Lavas. *Radiochim. Acta* **1993**, *60* (2–3), 149–152.
- (34) Keller, V. C. Untersuchungen Über Die Germanate Und Silikate Des Typs ABO_4 Der Vierwertigen Elemente Thorium Bis Americium. *Nukleonik* **1963**, No. 5, 41–48.
- (35) Estevenon, P.; Welcomme, E.; Tamain, C.; Jouan, G.; Szenknect, S.; Mesbah, A.; Poinssot, C.; Moisy, P.; Dacheux, N. Formation of PuSiO_4 under Hydrothermal Conditions. *Dalt. Trans.* **2020**, *49*, 6434–6445.
- (36) Hanchar, J. M.; Burakov, B. E.; Zamoryanskaya, M. V.; Garbuzov, V. M.; Kitsay, A. A.; Zirlin, V. A. Investigation of Pu Incorporation into Zircon Single Crystal. *Mater. Res. Soc. Symp. Proc.* **2004**, *824*, 225–229.
- (37) Ferriss, E. D. A.; Ewing, R. C.; Becker, U. Simulation of Thermodynamic Mixing Properties of Actinide-Containing Zircon Solid Solutions. *Am. Mineral.* **2010**, *95* (2–3), 229–241.
- (38) Zamoryanskaya, M. V.; Burakov, B. E. Feasibility Limits in Using Cerium as a Surrogate for Plutonium Incorporation in Zircon, Zirconia and Pyrochlore. *Mater. Res. Soc. Symp. - Proc.* **2000**, *663*, 301–306.
- (39) Putnam, R. L.; Navrotsky, A.; Cordfunke, E. H. P.; Huntelaar, M. E. Thermodynamics of Formation of Two Cerium Aluminum Oxides, $\text{CeAlO}_{3(s)}$ And $\text{CeAl}_{12}\text{O}_{19,918(s)}$ and Cerium Sesquioxide,

Ce₂O_{3(s)} At T= 298.15 K. *J. Chem. Thermodyn.* **2000**, *32* (7), 911–921.

(40) Putnam, R. L.; Gallegos, U. F.; Ebbinghaus, B. B.; Navrotsky, A.; Helean, K. B.; Ushakov, S. V.; Woodfield, B. F.; Boerio-Goates, J.; Williamson, M. A. Formation Energetics of Ceramic Phases Related to Surplus Plutonium Disposition. *Ceram. Trans.* **2001**, *119*, 147–158.

(41) Marra, J. C.; Cozzi, A. D.; Pierce, R. A.; Pareizs, J. M.; Jurgensen, A. R.; Missimer, D. M. Cerium as a Surrogate in the Plutonium Immobilized Form. In *Environmental Issues and Waste Management Technologies in the Ceramic and Nuclear Industries*; Smith, G. L., Sundaram, S. K., Spearing, D. R., Eds.; American Ceramic Society, 2002; pp 381–388.

(42) Shannon, R. D. Revised Effective Ionic Radii and Systematic Studies of Interatomic Distances in Halides and Chalcogenides. *Acta Crystallogr., Sect. A: Cryst. Phys., Diffraction, Theor. Gen. Crystallogr.* **1976**, *32* (5), 751–767.

(43) Estevenon, P.; Welcomme, E.; Szenknect, S.; Mesbah, A.; Moisy, P.; Poinssot, C.; Dacheux, N. Preparation of CeSiO₄ from Aqueous Precursors under Soft Hydrothermal Conditions. *Dalt. Trans.* **2019**, *48* (22), 7551–7559.

(44) Estevenon, P.; Kaczmarek, T.; Vadot, F.; Dumas, T.; Solari, P. L.; Welcomme, E.; Szenknect, S.; Mesbah, A.; Moisy, P.; Poinssot, C.; Dacheux, N. Formation of CeSiO₄ from Cerium (III) Silicate Precursors. *Dalton Trans.* **2019**, *48*, 10455–10463.

(45) Sverjensky, D. A.; Molling, P. A. A Linear Free Energy Relationship for Crystalline Solids and Aqueous Ions. *Nature* **1992**, *356* (6366), 231–234.

(46) Navrotsky, A. Systematic Trends and Prediction of Enthalpies of Formation of Refractory Lanthanide and Actinide Ternary Oxide Phases. *Ceram. Trans.* **2001**, No. 119, 137–146.

(47) Helean, K. B.; Navrotsky, A.; Lumpkin, G. R.; Colella, M.; Lian, J.; Ewing, R. C.; Ebbinghaus, B.; Catalano, J. G. Enthalpies of Formation of U-, Th-, Ce-Brannerite: Implications for Plutonium Immobilization. *J. Nucl. Mater.* **2003**, *320* (3), 231–244.

(48) Guo, X.; Szenknect, S.; Mesbah, A.; Labs, S.; Clavier, N.; Poinssot, C.; Ushakov, S. V.; Curtius, H.; Bosbach, D.; Ewing, R. C.; Burns, P. C.; Dacheux, N.; Navrotsky, A. Thermodynamics of Formation of Coffinite, USiO₄. *Proc. Natl. Acad. Sci. U. S. A.* **2015**, *112* (21), 6551–6555.

(49) Szenknect, S.; Mesbah, A.; Cordara, T.; Clavier, N.; Brau, H. P.; Le Goff, X.; Poinssot, C.; Ewing, R. C.; Dacheux, N. First Experimental Determination of the Solubility Constant of Coffinite. *Geochim. Cosmochim. Acta* **2016**, *181*, 36–53.

(50) Costin, D. T.; Mesbah, A.; Clavier, N.; Dacheux, N.; Poinssot, C.; Szenknect, S.; Ravoux, J. How to Explain the Difficulties in the Coffinite Synthesis from the Study of Uranothorite? *Inorg. Chem.* **2011**, *50* (21), 11117–11126.

(51) Frondel, C.; Collette, R. L. Hydrothermal Synthesis of Zircon, Thorite and Huttonite. *Am. Mineral.* **1957**, *42* (378), 759–765.

(52) Mumpton, F. A.; Roy, R. Hydrothermal Stability Studies of the Zircon-Thorite Group. *Geochim. Cosmochim. Acta* **1961**, *21* (3–4), 217–238.

(53) Estevenon, P.; Welcomme, E.; Szenknect, S.; Mesbah, A.; Moisy, P.; Poinssot, C.; Dacheux, N. Impact of Carbonate Ions on the Synthesis of ThSiO₄ under Hydrothermal Conditions. *Inorg. Chem.* **2018**, *57* (19), 12398–12408.

(54) Estevenon, P.; Welcomme, E.; Szenknect, S.; Mesbah, A.; Moisy, P.; Poinssot, C.; Dacheux, N. Multiparametric Study of the Synthesis of ThSiO₄ under Hydrothermal Conditions. *Inorg. Chem.* **2018**, *57* (15), 9393–9402.

(55) Schlüter, J.; Malcherek, T.; Husdal, T. A. The New Mineral Stetindite, CeSiO₄, a Cerium End-Member of the Zircon Group. *Neues Jahrb. Mineral., Abh.* **2009**, *186* (2), 195–200.

(56) Navrotsky, A.; Kleppa, O. J. A Calorimetric Study of Molten Na₂MoO₄-MoO₃ Mixtures at 970 K. *Inorg. Chem.* **1967**, *6* (11), 2119–2121.

(57) Navrotsky, A. Progress and New Directions in High Temperature Calorimetry. *Phys. Chem. Miner.* **1977**, *2*, 89–104.

(58) Navrotsky, A. Progress and New Directions in Calorimetry: A 2014 Perspective. *J. Am. Ceram. Soc.* **2014**, *97* (11), 3349–3359.

(59) Ushakov, S. V.; Helean, K. B.; Navrotsky, A.; Boatner, L. A. Thermochemistry of Rare-Earth Orthophosphates. *J. Mater. Res.* **2001**, *16* (9), 2623–2633.

(60) Helean, K. B.; Navrotsky, A. Oxide Melt Solution Calorimetry of Rare Earth Oxides. Techniques, Problems, Cross-Checks, Successes. *J. Therm. Anal. Calorim.* **2002**, *69* (3), 751–771.

(61) Guo, X.; Boukhalfa, H.; Mitchell, J. N.; Ramos, M.; Gaunt, A. J.; Migliori, A.; Roback, R. C.; Navrotsky, A.; Xu, H. Sample Seal-and-Drop Device and Methodology for High Temperature Oxide Melt Solution Calorimetric Measurements of PuO₂. *Rev. Sci. Instrum.* **2019**, *90* (4), 044101.

(62) Gorman-Lewis, D.; Mazeina, L.; Fein, J. B.; Szymanowski, J. E. S.; Burns, P. C.; Navrotsky, A. Thermodynamic Properties of Soddyite from Solubility and Calorimetry Measurements. *J. Chem. Thermodyn.* **2007**, *39* (4), 568–575.

(63) Navrotsky, A.; Shvareva, T.; Guo, X. Thermodynamics of Uranium Minerals and Related Materials. *Mineralogical Association of Canada Short Course* **2013**, *43*, 1–18.

(64) Guo, X.; Tiferet, E.; Qi, L.; Solomon, J. M.; Lanzirrotti, A.; Newville, M.; Engelhard, M. H.; Kukkadapu, R. K.; Wu, D.; Ilton, E. S.; Asta, M.; Sutton, S. R.; Xu, H.; Navrotsky, A. U(v) in Metal Uranates: A Combined Experimental and Theoretical Study of MgUO₄, CrUO₄, and FeUO₄. *Dalt. Trans.* **2016**, *45* (11), 4622–4632.

(65) Guo, X.; Wu, D.; Xu, H.; Burns, P. C.; Navrotsky, A. Thermodynamic Studies of Studtite Thermal Decomposition Pathways via Amorphous Intermediates UO₃, U₂O₇, and UO₄. *J. Nucl. Mater.* **2016**, *478*, 158–163.

(66) Clavier, N.; Szenknect, S.; Costin, D. T.; Mesbah, A.; Poinssot, C.; Dacheux, N. From Thorite to Coffinite: A Spectroscopic Study of Th_{1-x}U_xSiO₄ Solid Solutions. *Spectrochim. Acta, Part A* **2014**, *118*, 302–307.

(67) Speer, J. A.; Cooper, B. J. Crystal Structure of Synthetic Hafnon, HfSiO₄, Comparison with Zircon and the Actinide Orthosilicates. *Am. Mineral.* **1982**, *67* (7–8), 804–808.

(68) Janeczek, J.; Ewing, R. C. Coffinitization - A Mechanism for the Alteration of UO₂ under Reducing Conditions. *MRS Proc.* **1991**, *257*, 257.

(69) Finch, R.; Murakami, T. Systematics and Paragenesis of Uranium Minerals. In *Uranium: Mineralogy, Geochemistry, and the Environment*; Burns, P. C., Finch, R. J., Eds.; De Gruyter, 1999; pp 91–179. DOI: 10.1515/9781501509193-008

(70) Janeczek, J. Composition and Origin of Coffinite from Jachymov, Czechoslovakia. *Neues Jahrb. Mineral., Abh.* **1991**, *9*, 385–395.

(71) Nasdala, L.; Beran, A.; Libowitzky, E.; Wolf, D. The Incorporation of Hydroxyl Groups and Molecular Water in Natural Zircon (ZrSiO₄). *Am. J. Sci.* **2001**, *301* (10), 831–857.

(72) Miller, F. A.; Wilkins, C. H. Infrared Spectra and Characteristic Frequencies of Inorganic Ions. *Anal. Chem.* **1952**, *24* (8), 1253–1294.

(73) Speer, J. A. Zircon. *Rev. Mineral. Geochem.* **1982**, *5*, 66–112.

(74) Labs, S.; Hennig, C.; Weiss, S.; Curtius, H.; Zänker, H.; Bosbach, D. Synthesis of Coffinite, USiO₄, and Structural Investigations of U_xTh_(1-x)SiO₄ Solid Solutions. *Environ. Sci. Technol.* **2014**, *48* (1), 854–860.

(75) Hirono, T.; Tanikawa, W. Implications of the Thermal Properties and Kinetic Parameters of Dehydroxylation of Mica Minerals for Fault Weakening, Frictional Heating, and Earthquake Energetics. *Earth Planet. Sci. Lett.* **2011**, *307* (1–2), 161–172.

(76) Perrillat, J. P.; Daniel, I.; Koga, K. T.; Reynard, B.; Cardon, H.; Crichton, W. A. Kinetics of Antigorite Dehydration: A Real-Time X-Ray Diffraction Study. *Earth Planet. Sci. Lett.* **2005**, *236* (3–4), 899–913.

(77) Tavakoli, A. H.; Maram, P. S.; Widgeon, S. J.; Rufner, J.; Van Benthem, K.; Ushakov, S.; Sen, S.; Navrotsky, A. Amorphous Alumina Nanoparticles: Structure, Surface Energy, and Thermodynamic Phase Stability. *J. Phys. Chem. C* **2013**, *117* (33), 17123–17130.

- (78) Levchenko, A. A.; Li, G.; Boerio-Goates, J.; Woodfield, B. F.; Navrotsky, A. TiO_2 Stability Landscape: Polymorphism, Surface Energy, and Bound Water Energetics. *Chem. Mater.* **2006**, *18* (26), 6324–6332.
- (79) Ushakov, S. V.; Navrotsky, A. Direct Measurements of Water Adsorption Enthalpy on Hafnia and Zirconia. *Appl. Phys. Lett.* **2005**, *87* (16), 164103.
- (80) Chen, F.; Ewing, R. C.; Clark, S. B. The Gibbs Free Energies and Enthalpies of Formation of U^{6+} Phases: An Empirical Method of Prediction. *Am. Mineral.* **1999**, *84* (4), 650–664.
- (81) Xu, H.; Wang, Y.; Barton, L. L. Application of a Linear Free Energy Relationship to Crystalline Solids of MO_2 and $\text{M}(\text{OH})_4$. *J. Nucl. Mater.* **1999**, *273* (3), 343–346.
- (82) Xu, H.; Wang, Y. Use of Linear Free Energy Relationship to Predict Gibbs Free Energies of Formation of Pyrochlore Phases (CaMTi_2O_7). *J. Nucl. Mater.* **1999**, *275* (2), 216–220.
- (83) Navrotsky, A. Thermochemical Insights into Refractory Ceramic Materials Based on Oxides with Large Tetravalent Cations. *J. Mater. Chem.* **2005**, *15* (19), 1883–1890.
- (84) Qi, J.; Guo, X.; Mielewicz-Gryn, A.; Navrotsky, A. Formation Enthalpies of LaLnO_3 (Ln = Ho, Er, Tm and Yb) Interlanthanide Perovskites. *J. Solid State Chem.* **2015**, *227*, 150–154.
- (85) Helean, K. B.; Ushakov, S. V.; Brown, C. E.; Navrotsky, A.; Lian, J.; Ewing, R. C.; Farmer, J. M.; Boatner, L. A. Formation Enthalpies of Rare Earth Titanate Pyrochlores. *J. Solid State Chem.* **2004**, *177* (6), 1858–1866.
- (86) Cotton, S. *Lanthanide and Actinide Chemistry*; John Wiley & Sons, Ltd., 2006.
- (87) Seaborg, G. T. The Transuranium Elements. *Science* **1946**, *104* (2704), 379–386.
- (88) Seaborg, G. T. Origin of the Actinide Concept. In *Handbook on the Physics and Chemistry of Rare Earths*; Gschneidner, K. A., Eyring, L. J., Choppin, G. R., Lander, G. H., Eds.; Elsevier B.V., 1994; Vol. 18, pp 1–26. DOI: 10.1016/S0168-1273(05)80041-8
- (89) Silver, M. A.; Albrecht-Schmitt, T. E. Evaluation of f-Element Borate Chemistry. *Coord. Chem. Rev.* **2016**, *323*, 36–51.
- (90) Albrecht-Schmitt, T. E. *Organometallic and Coordination Chemistry of the Actinides*; Springer, 2012. DOI: 10.1093/ntr/nts065
- (91) Horne, G. P.; Grimes, T. S.; Bauer, W. F.; Dares, C. J.; Pimblott, S. M.; Mezyk, S. P.; Mincher, B. J. Effect of Ionizing Radiation on the Redox Chemistry of Penta- And Hexavalent Americium. *Inorg. Chem.* **2019**, *58* (13), 8551–8559.
- (92) Sullivan, J. C.; Gordon, S.; Mulac, W. A.; Schmidt, K. H.; Cohen, D.; Sjoblom, R. Pulse Radiolysis Studies of Americium(III) and Curium(III) Ions in Perchlorate Media. The Preparation of Am II, Am IV, Cm II and Cm IV. *Inorg. Nucl. Chem. Lett.* **1976**, *12* (8), 599–601.
- (93) Keenan, T. K. Americium and Curium. *J. Chem. Educ.* **1959**, *36* (1), 27–31.
- (94) *The Chemistry of the Actinides and Transactinide Elements*, 4th ed.; Morss, L. R., Edelstein, N. M., Fuger, J., Eds.; Springer: Dordrecht, The Netherlands, 2010.
- (95) White, F. D.; Dan, D.; Albrecht-Schmitt, T. E. Contemporary Chemistry of Berkelium and Californium. *Chem. - Eur. J.* **2019**, *25* (44), 10251–10261.
- (96) Mincher, B. J.; Martin, L. R.; Schmitt, N. C. Diamylamylphosphonate Solvent Extraction of Am(VI) from Nuclear Fuel Raffinate Simulant Solution. *Solvent Extr. Ion Exch.* **2012**, *30* (5), 445–456.
- (97) Keenan, T. K. First Observation of Aqueous Tetravalent Curium. *J. Am. Chem. Soc.* **1961**, *83* (17), 3719–3720.
- (98) Guo, X.; Xu, H. Enthalpies of Formation of Polyhalite: A Mineral Relevant to Salt Repository. *J. Chem. Thermodyn.* **2017**, *114*, 44–47.
- (99) Xu, H.; Guo, X.; Bai, J. Thermal Behavior of Polyhalite: A High-Temperature Synchrotron XRD Study. *Phys. Chem. Miner.* **2017**, *44* (2), 125–135.
- (100) Timofeev, A.; Migdisov, A. A.; Williams-Jones, A. E.; Roback, R.; Nelson, A. T.; Xu, H. Uranium Transport in Acidic Brines under Reducing Conditions. *Nat. Commun.* **2018**, *9* (1), 2–8.
- (101) Fox, P. M.; Tinnacher, R. M.; Cheshire, M. C.; Caporuscio, F.; Carrero, S.; Nico, P. S. Effects of Bentonite Heating on U(VI) Adsorption. *Appl. Geochem.* **2019**, *109*, 104392.
- (102) Utsunomiya, S.; Kersting, A. B.; Ewing, R. C. Groundwater Nanoparticles in the Far-Field at the Nevada Test Site: Mechanism for Radionuclide Transport. *Environ. Sci. Technol.* **2009**, *43* (5), 1293–1298.
- (103) Novikov, A. P.; Kalmykov, S. N.; Utsunomiya, S.; Ewing, R. C.; Horreard, F.; Merkulov, A.; Clark, S. B.; Tkachev, V. V.; Myasoedov, B. F. Colloid Transport of Plutonium in the Far-Field of the Mayak Production Association, Russia. *Science (Washington, DC, U. S.)* **2006**, *314* (5799), 638–641.
- (104) Dittrich, T. M.; Boukhalfa, H.; Ware, S. D.; Reimus, P. W. Laboratory Investigation of the Role of Desorption Kinetics on Americium Transport Associated with Bentonite Colloids. *J. Environ. Radioact.* **2015**, *148*, 170–182.
- (105) Estevenon, P.; Causse, J.; Szenknect, S.; Welcomme, E.; Mesbah, A.; Moisy, P.; Poinssot, C.; Dacheux, N. In-Situ Study of the Synthesis of Thorite (ThSiO_4) under Environmental Representative Conditions. *Dalt. Trans.* **2020**, *49*, 11512–11521.
- (106) Mesbah, A.; Szenknect, S.; Clavier, N.; Lozano-Rodriguez, J.; Poinssot, C.; Den Auwer, C.; Ewing, R. C.; Dacheux, N. Coffinite, USiO_4 , Is Abundant in Nature: So Why Is It So Difficult to Synthesize? *Inorg. Chem.* **2015**, *54* (14), 6687–6696.
- (107) Konings, R. J. M.; Beneš, O.; Kovács, A.; Manara, D.; Sedmidubský, D.; Gorokhov, L.; Iorish, V. S.; Yungman, V.; Shenyavskaya, E.; Osina, E. The Thermodynamic Properties of the f-Elements and Their Compounds: Part 2. The Lanthanide and Actinide Oxides. *J. Phys. Chem. Ref. Data* **2014**, *43* (1), 013101.
- (108) Dorogova, M.; Navrotsky, A.; Boatner, L. A. Enthalpies of Formation of Rare Earth Orthovanadates, REVO_4 . *J. Solid State Chem.* **2007**, *180* (3), 847–851.
- (109) Polinski, M. J.; Garner, E. B.; Maurice, R.; Planas, N.; Stritzinger, J. T.; Parker, T. G.; Cross, J. N.; Green, T. D.; Alekseev, E. V.; Van Cleve, S. M.; Depmeier, W.; Gagliardi, L.; Shatruck, M.; Knappenberger, K. L.; Liu, G.; Skanthakumar, S.; Soderholm, L.; Dixon, D. A.; Albrecht-Schmitt, T. E. Unusual Structure, Bonding and Properties in a Californium Borate. *Nat. Chem.* **2014**, *6* (5), 387–392.
- (110) Mazeina, L.; Ushakov, S. V.; Navrotsky, A.; Boatner, L. A. Formation Enthalpy of ThSiO_4 and Enthalpy of the Thorite \rightarrow Huttonite Phase Transition. *Geochim. Cosmochim. Acta* **2005**, *69* (19), 4675–4683.
- (111) Estevenon, P.; Kaczmarek, T.; Rafiuddin, M. R.; Welcomme, E.; Szenknect, S.; Mesbah, A.; Moisy, P.; Poinssot, C.; Dacheux, N. Soft Hydrothermal Synthesis of Hafnon, HfSiO_4 . *Cryst. Growth Des.* **2020**, *20*, 1820.
- (112) Suchanek, W. L.; Riman, R. E. Hydrothermal Synthesis of Advanced Ceramic Powders. *Adv. Sci. Technol.* **2006**, *45*, 184–193.
- (113) Weber, W. J.; Ewing, R. C.; Catlow, C. R. A.; Diaz De La Rubia, T.; Hobbs, L. W.; Kinoshita, C.; Matzke, H.; Motta, A. T.; Nastasi, M.; Salje, E. K. H.; Vance, E. R.; Zinkle, S. J. Radiation Effects in Crystalline Ceramics for the Immobilization of High-Level Nuclear Waste and Plutonium. *J. Mater. Res.* **1998**, *13* (6), 1434–1484.
- (114) Weber, W. J.; Ewing, R. C.; Wang, L. M. The Radiation-Induced Crystalline-to-Amorphous Transition in Zircon. *J. Mater. Res.* **1994**, *9* (3), 688–698.
- (115) Murakami, T.; Chakoumakos, B. C.; Ewing, R. C.; Lumpkin, G. R.; Weber, W. J. Alpha-Decay Event Damage in Zircon. *Am. Mineral.* **1991**, *76*, 1510–1532.
- (116) Ewing, R. C. Displaced by Radiation. *Nature* **2007**, *445*, 161–162.
- (117) Weber, W. J. Self-Radiation Damage and Recovery in P-Doped Zircon. *Radiat. Eff. Defects Solids* **1991**, *115* (4), 341–349.
- (118) Farnan, I.; Cho, H.; Weber, W. J. Quantification of Actinide α -Radiation Damage in Minerals and Ceramics. *Nature* **2007**, *445* (7124), 190–193.

(119) Robie, R. A.; Hemingway, B. S. Thermodynamic Properties of Minerals and Related Substances at 298.15 K and 1 bar (105 Pascals) Pressure and at Higher Temperatures. *U.S. Geol. Surv. Bull.* **1995**, 2131.

(120) Navrotsky, A.; Ushakov, S. V. *Materials Fundamentals of Gate Dielectrics*; Springer, 2005.